EMPIR EURAMET
The EMPIR initiative is co-funded by the European Union's Horizon 2020 research and innovation programme and the EMPIR Participating States

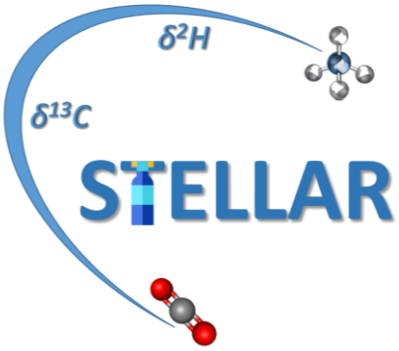

19ENV05 STELLAR

(Stable isotope metrology to enable climate action and regulation)

D6

Good practice guide for accurate methane isotope ratio measurements using laser spectroscopy: analyser characterisation and statement of uncertainty with a target precision of 0.2 ‰ for $\delta^{13}C$ (CH_4) and 1 ‰ for $\delta\ ^{2}H$ $(CH)_4$.

Coordinator	Paul Brewer (NPL)
Authors:	Chris Rennick (NPL), Tim Arnold (NPL), Cam Yeo (NPL), Joachim Mohn (Empa), Kerstin Zeyer (Empa), Jelka Braden-Behrens (PTB), Volker Ebert (PTB), Anas Emad (PTB), Gang Li (PTB), Javis Nwaboh (PTB), Olav Werhahn (PTB), Stefan Persijn (VSL), Mehr Fatima (VTT), Thomas Hausmaninger (VTT), Heike Geilmann (BGC-IsoLab), Heiko Moossen (BCG-IsoLab)

NPL: National Physical Laboratory, Hampton Road, Teddington, UK
BCG-IsoLab: Stable Isotope Laboratory (BGC-IsoLab), Max-Planck-Institute for Biogeochemistry, Hans-Knoell-Str. 10, 07745 Jena, Germany
EMPA: Eidgenoessische Materialpruefungs- und Forschungsanstalt, Ueberlandstrasse 129, CH-8600 Duebendorf, Switzerland,
PTB: Physikalisch-Technische Bundesanstalt (PTB), Bundesallee 100, 38116 Braunschweig, Germany
VSL: Thijsseweg 11, 2629 JA Delft, the Netherlands
VTT: Teknologian tutkimuskeskus VTT Oy, Vuorimiehentie 3, 02044 VTT, 1000, Espoo, Finland

Due Date: Feb 2023 (M30)

Submission Date: Oct 2023

Contents

This project has received funding from the EMPIR Programme co-financed by the Participating States and from the European Union's Horizon 2020 research and innovation program.

1 Introduction

Methane (CH_4) is the second most important anthropogenic greenhouse gas after carbon dioxide (CO_2) (Canadell et al., 2021). The amount fraction in the atmosphere is growing with the rate of change varying over the observation record and a more rapid growth starting in 2007 (Nisbet et al., 2019). Simultaneous measurement of the stable isotope ratios can provide insight into the relative magnitudes of the various sources and sinks and have been performed at global background sites (Nisbet et al., 2016; Miller et al., 2002) and regional atmospheric monitoring stations (Röckmann et al., 2016). These measurements have been performed by isotope ratio mass spectrometry (IRMS), but ease of use, sampling frequency and improving precision has led to a growth in deployment of optical isotope ratio spectrometers (OIRS) based on techniques such as Fourier transform spectroscopy (FTIR) (Griffith et al., 2012; Flores et al., 2017), cavity ringdown spectroscopy (CRDS) (Rella et al., 2015; Miles et al., 2018; Saboya et al., 2022), and tuneable infrared laser direct absorption spectroscopy (TILDAS) (Santoni et al., 2012; Eyer et al., 2016; Rennick et al., 2021).

The absorption of infrared light by molecular gases is a well-established method to quantify the amount fraction of these gases in a mixture. Different species absorb light in distinctive regions of the spectrum, providing selectivity, and the absorbance is in proportion to the abundance, providing quantification. This technique to quantify stable isotope ratios in CH_4 by direct measurement of the amount fraction of individual isotopologues – $^{12}CH_4$, $^{13}CH_4$ and $^{12}CH_3D$ – then taking the ratio of these amount fractions in a similar manner to isotope ratio mass spectrometry (IRMS). The isotope ratios are calculated as:

$$\delta^{13}\mathrm{C}\ (\mathrm{CH_4}) = \frac{Y_{311}^{\mathrm{samp}} \Big/ Y_{211}^{\mathrm{samp}}}{{}^{13}r_{\mathrm{ref}}} - 1 \tag{1}$$

$$\delta\ {}^{2}\mathrm{H}\ (\mathrm{CH_4}) = \frac{Y_{212}^{\mathrm{samp}} \Big/ Y_{211}^{\mathrm{samp}}}{4\ {}^{2}r_{\mathrm{ref}}} - 1 \tag{2}$$

where the amount fraction Y of the isotopologues are labelled by the AFGL notation $Y_{211} \equiv Y\left({}^{12}\mathrm{CH_4}\right)$, $Y_{311} \equiv Y\left({}^{13}\mathrm{CH_4}\right)$ and $Y_{212} \equiv Y\left({}^{12}\mathrm{CH_3D}\right)$ (Gordon et al., 2022). ${}^{13}r_{\mathrm{ref}} = 0.011180$ and ${}^{2}r_{\mathrm{ref}} = 0.00015575$ are the reference isotope ratios of VPDB and VSMOW respectively (Werner and Brand, 2001).

A requirement for the atmospheric measurements is that the calibrated isotope ratios are traceable to the same reference materials as IRMS measurements to allow comparison between sites and across time series. Targeted precisions have been identified by the Global Atmospheric Watch (GAW) for well-mixed background air and source studies, where this is a measure of the bias between different measurement networks. From this for the STELLAR project target precisions of 0.2‰ for δ ^{13}C and 1‰ for δ ^{2}H, were derived.

2 Spectroscopic Characterisation

Performance of OIRS instruments for isotope deltas are limited by several factors, which are partly specific to optical measurements (e.g. line data), while others also apply to IRMS (matrix effects, etc.). In this project the following limitations have been investigated:

Matrix Effect	Differences in the gas composition of the matrix of the CH_4 sample and the calibration standard can lead to a bias in reported isotope ratio due to pressure broadening of the measured absorption lines.
Spectral interferences	Differences in the trace gas composition of the CH_4 sample and the calibration standard can lead to a bias due to spectral overlap of the trace species and the measured lines of the CH_4 isotopologues.
CH_4 amount fraction changes	Differences in the CH_4 amount fraction between the sample and the calibration standard can lead to a bias due to changes in the isotopologue amount fraction ratio reported by the spectrometer software.
Isotopic signature of reference materials	Large differences in the isotopic signature between the sample and the available reference materials can require large extrapolation.
Abundance	Low abundance of rare isotopologues limit signal strengths and the analytical precision.
Line data	Uncertainties in the tabulated data that relate the shape of an absorption signal may translate to uncertainty in the amount fraction in a similar manner as the matrix effect.

2.1 Measurement and fitting the spectrum

The spectrometer used in the NPL pre-concentrator system is a commercial tuneable infrared laser direct absorption spectrometer (TILDAS) manufactured by Aerodyne Research Inc., Billerica MA. The instrument uses a multi-pass cell with a nominal volume of 500 cm^3 to contain the sample with an absorption path length of 76 m. The spectrum is recorded by scanning the wavelength of two mid infrared quantum cascade lasers while recording the intensity transmitted through the cell. Software (TDLWintel) controls the data acquisition and fitting the spectrum for the amount fraction of each isotopologues. An example of a spectrum and its fit is shown in Figure 1.

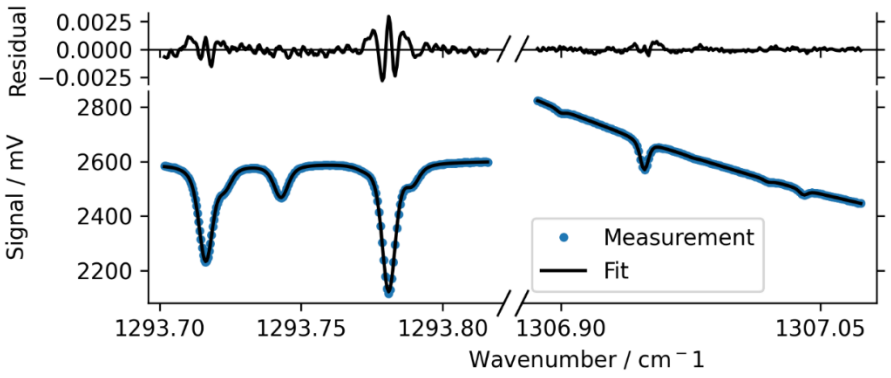

Figure 1 Spectrum recorded by a TILDAS dual laser system of a sample of 500 µmol mol^{-1} CH_4 in N_2. The points are the measured laser transmission through the 76 m path length cell, the solid line is a fit to the spectroscopic absorption with a polynomial baseline.

The fit to the spectrum represents each absorption as a Voigt function where the area is proportional to the amount fraction and the width proportional to temperature and pressure, and the background is a polynomial function that represents the variation of laser intensity with wavelength. For computational efficiency, the instrument fits only for amount fraction and baseline, with the other peak shape parameters calculated from the measured temperature and pressure using the broadening parameters listed in the Hitran database. These parameters will contribute to the uncertainty of fitting directly from the uncertainty on the values, and indirectly as the parameters are given for a nominal "air" gas composition. The presence of other gases can result in a bias to the fitted amount fraction that is often termed the "gas matrix effect". Differences between the true amount fraction of the sample and the value reported by the spectrometer can be minimised by a suitable calibration scheme, but it is important that the matrix of the standard and sample are well matched, which is discussed in section 0. The amount fraction is calculated from the fitted peak area using the Hitran spectral line data for the absorption coefficient, which is scaled by the nominal abundance.

2.2 Limit of detection

As the focus of the STELLAR project was on the study of isotopologues in atmospheric CH_4, subject to CH_4 additions from adjacent sources no measurements at lower amount fractions (i.e., below 1.8 µmol mol^{-1}) were conducted. The limit of detection, however, would be relevant for analysis of air depleted in CH_4, for example by partial oxidation or stratospheric destruction.

2.3 Instrument stability (Allan variance and temperature stability)

The sample for a spectroscopic measurement is loaded into the optical cell, typically at a below-ambient pressure that is controlled by the spectrometer, then the spectrum is accumulated over some length of time. The gas can either flow continuously, so that the sample is refreshed, or loaded into the cell and isolated by closing valves to trap the sample. The latter is the mode of operation used for preconcentrator systems as the preconcentration step is also a batch process. In either case there is an optimum duration over which to record the spectrum – where the averaging improves the signal to noise ratio – that can be identified using the Allan-Werle variance (Werle et al., 2004; Werle, 2011). The procedure to quantify this is to record the instrument response over an extended time, then process this with varying averaging durations. The steps are to split the data into M sub-groups (i.e. with integration time $\tau = T/M$ where T is the duration of the complete dataset), then calculate the variance between pairs of successive subgroups. The variance is then given by (Werle, 2011):

$$\sigma^2(\tau) = \frac{1}{M-1}\sum_{i=1}^{M-1}\frac{(\overline{y_{i+1}} - \overline{y_i})^2}{2} \qquad (3)$$

This is repeated for different values of τ then plotted to visually identify the behaviour over increasing integration intervals.

Figure 2 shows measurements of a 550 µmol mol^{-1} sample of CH_4 in N_2 loaded to 2800 Pa into an Aerodyne spectrometer cell then held for 30 hours. The Allan-Werle analysis shows an optimal averaging duration of 100 s, during which random noise is the dominant source of variability and the averaging improves the measurement uncertainty. After 100 s instrumental drift begins to dominate, and the Allan deviation begins to increase. The source of drift in the case of this specific spectrometer is leakage of ambient air into the cell. This leak rate is small and within the manufacturer specifications but dilutes the sample.

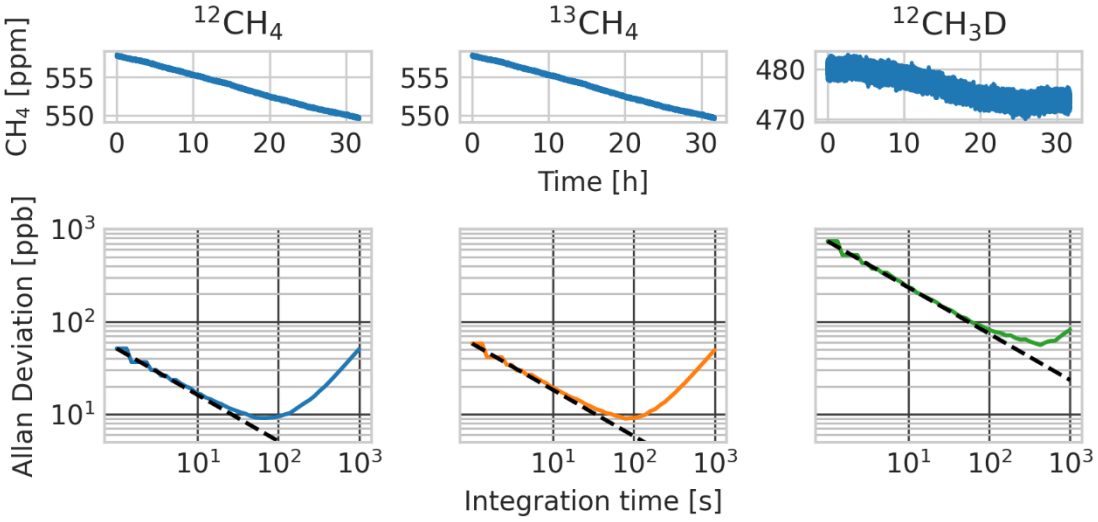

Figure 2 Continuous measurement of the same sample of 550 µmol mol−1 CH4 in N2 over 30 hours. The measurement is the uncalibrated amount fraction reported by the spectrometer and has been scaled by the nominal abundance of the isotopologue. The top plots show the instrument response, and the lower plots are the same data processed for the Allan-Werle deviation. The dotted line in the lower three plots show the lower limit for random noise.

2.4 Amount fraction dependency of isotope ratio

Changes in the CH_4 amount fraction may produce feedback on apparent isotope delta values due to a non-linear response of the analyser on changes in isotopologue amount fraction, this is often referred to as 'linearity calibration'. The size of the effect depends on multiple parameters, including cell conditions (pressure, temperature, etc.), laser and data analysis software (laser line width, fitting procedure, background correction etc.). In an exemplary study the amount fraction dependency of the TIDLAS instrument at Empa was tested under conditions anticipated for future use of the instrument (Figure 3). The gases and setup applied was similar to the system in Figure 4.

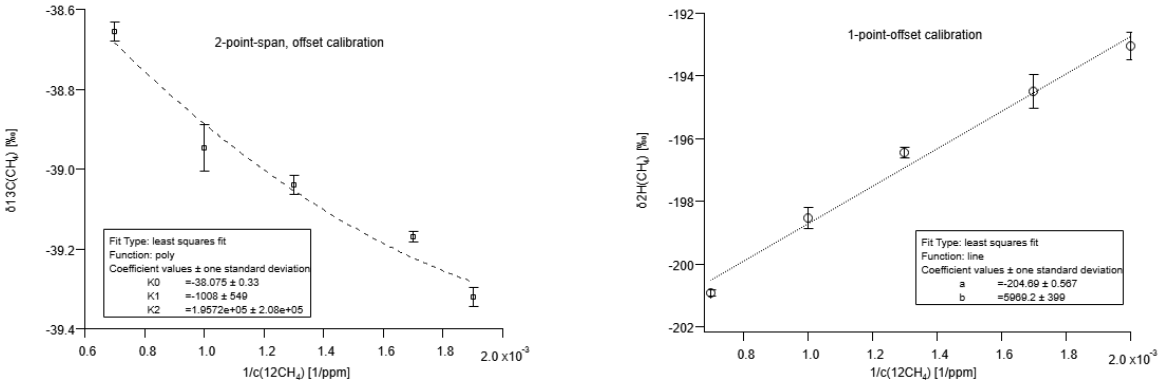

Figure 3 Apparent δ ^{13}C (CH_4) (left) and δ ^{2}H (CH_4) (right) as a function of inverse CH_4 amount fraction

2.5 Matrix gas effects

Changes in the gas matrix (O_2, N_2, Ar, H_2O, etc.) from standard ambient air composition that is reported in the HITRAN database causes variations in the pressure broadening coefficient effectively acting on the spectrum. This often results in a bias when fitting the spectrum with standard commercial fitting

software or typical spectrometers' firmware (an effect sometimes called 'gas matrix effect'). Matrix effects cancel out when the sample and the reference gas have similar gas matrix composition but are relevant when one or both deviates. One example is incomplete separation of a non-target gas species in CH_4 preconcentration. Therefore, incomplete gas species separation should be tested during instrumental developments and critical levels of gas matrix changes should be evaluated.

Within STELLAR matrix effects of oxygen (O_2 from 0% to around 20%), argon (Ar from 0% to around 1%) and krypton (Kr from 0 µmol mol^1 to around 4000 µmol mol^1) on apparent $\delta^{13}C(CH_4)$ and $\delta^{2}H(CH_4)$ values were tested for the TILDAS spectrometer at Empa. The experimental setup is shown in Figure 4 and exemplary results are provided in Figure 5. Findings of our study demonstrate, that in order to limit effects on $\delta\ ^{13}C\ (CH_4)$ and $\delta\ ^{2}H\ (CH_4)$ below 0.2‰ and 5‰, respectively, the following preventions have to be met: O_2 has to be removed to better than 1.4% in order to limit effects to 0.2‰ for $\delta\ ^{13}C\ (CH_4)$, while the O_2 gas matrix effect is less severe for $\delta\ ^{2}H\ (CH_4)$. For both Ar and Kr, effects are strongest on $\delta\ ^{2}H\ (CH_4)$, where 17% of Ar or 24% of Kr result in deviations of 5‰, while observed changes were lower for $\delta\ ^{13}C\ (CH_4)$.

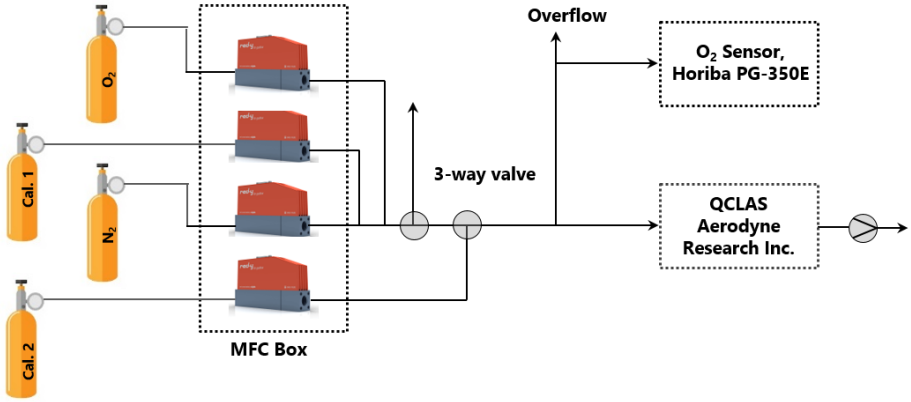

Figure 4 Setup established at Empa to characterise O_2, Ar, and Kr gas matrix effects on apparent $\delta\ ^{13}C\ (CH_4)$ and $\delta\ ^{2}H\ (CH_4)$ values. An additional oxygen sensor was applied to verify dynamic O_2 dilution using mass flow controllers (MFC). The following gases were applied: Calibration gas 1 with $C(CH_4)$ = 10,000 µmol mol^{-1}, Calibration gas 2 with $C(CH_4)$ = 569 µmol mol^{-1}, N_2 purity 99.9999%, O_2 purity 99.9999%. For the Ar and Kr experiments the O_2 cylinder was replaced by 1.999 % Ar in N_2 or 5005 ± 50 µmol mol^{-1} Kr in N_2.

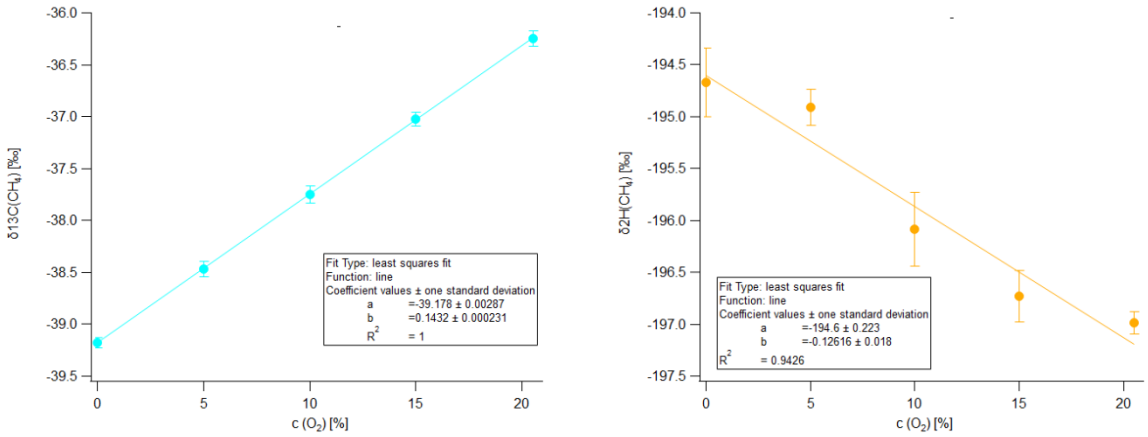

Figure 5 Changes of apparent $\delta\ ^{13}C(CH_4)$ (left) and $\delta\ ^{2}H(CH_4)$ (right) values as a function of O_2 concentration in the N_2 gas matrix.

2.6 Spectral interferences

The presence of additional trace gases, which are not spectrally resolved, can yield changes in the apparent isotopologue concentrations and delta values if they are not separated prior to analysis.

Interfering substances can be identified using the HITRAN or other spectral databases. A database survey was conducted for the spectral regions used by partners in the Stellar project and potential interfering species are listed in Appendix B.

For the specific Empa TILDAS analyser, critical levels of major interferences, nitrous oxide (N_2O) and water vapour (H_2O), were determined. For N_2O interference tests, a gaseous standard (480 ± 42 nmol mol^{-1} N_2O in N_2) in a setup similar to Figure 4 was used, while for H_2O a VOC calibration device (HovaCAL N424-VOC4) was used and H_2O concentration confirmed with a dew point meter. N_2O interferences are shown in Figure 6, indicating that 50 nmol mol^{-1} N_2O result in a 5‰ deviation for δ ^{2}H (CH_4), while the effect on δ ^{13}C (CH_4) is less pronounced. Water vapour must be removed to below 1200 µmol mol^{-1} to reach the extended WMO-GAW compatibility goals. The effect is more pronounced for δ ^{2}H (CH_4) than for δ ^{13}C (CH_4).

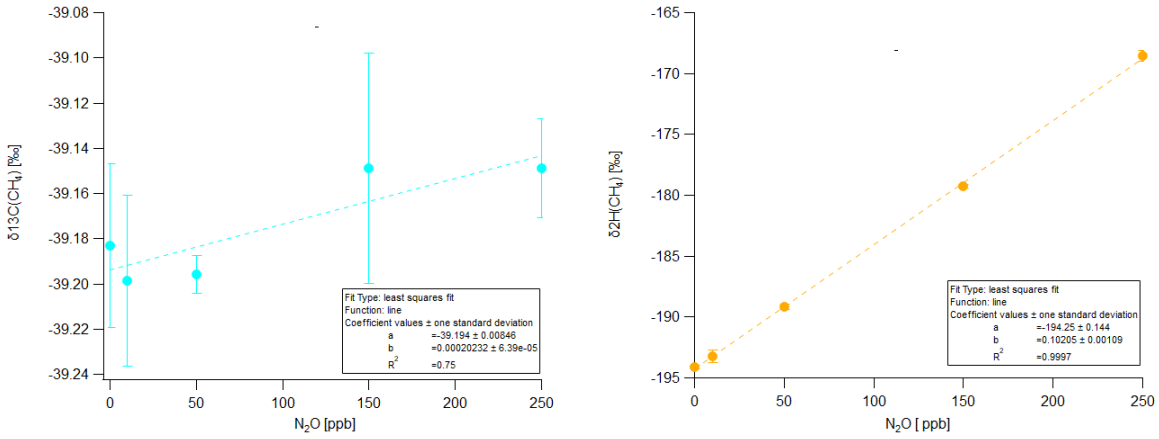

Figure 6 Apparent δ ^{13}C (CH_4) (left) and δ ^{2}H (CH_4) (right) values as a function of N_2O concentration in the gas mixture.

3 Calibration of isotope ratio spectrometers

The OIRS spectrometers must be calibrated using reference materials that are traceable to the international standard isotope references of VPDB for $^{13}C/_{12}C$ and VSMOW for $^{2}H/_{1}H$ (Werner and Brand, 2001). For most CH_4 samples with naturally-occurring abundances of all isotopologues these isotope ratios are equal to the isotopologue ratios – e.g., $^{13}C/_{12}C \approx Y(^{13}CH_4)/Y(^{12}CH_4)$ – to the limit of precision of OIRS or IRMS, so the calibration procedures here calibrate the spectrometer response. Preparation of these reference materials in a form suitable for spectrometer calibration is described in section 0.

The two general calibration approaches are described here: calibrating the instrument for isotopologue amount fraction, then calculating the ratio of these; and calibrating the isotopologue ratio.

3.1 Isotopologue amount fraction calibration

The pre-concentrator system at NPL uses a high-resolution dual-laser direct absorption spectrometer (Aerodyne Research, Inc., TILDAS-FD-L2) scanning around 1293.7 cm^{-1} to record $^{12}CH_4$ and $^{13}CH_4$ absorption and 1306.9 cm^{-1} to record $^{12}CH_3D$ absorption. The spectrum is fitted for a nominal amount fraction of each isotopologue using parameters from the Hitran2016 database, then these instrument responses are calibrated using two primary reference materials prepared using a single pure CH_4 parent

in a nitrogen (N_2) matrix that bracket the sample in amount fraction. The calibration follows the isotopologue amount fraction approach, where the spectrometer response to each isotopologue is calibrated then the isotopologue ratio is calculated from the ratio of these calibrated values. The isotopologue calibration method has been applied to CO_2 FTIR spectrometers (Griffith et al., 2012; Griffith, 2018; Flores et al., 2017) and TILDAS for CO_2 and CH_4 (Rennick et al., 2021; Steur et al., 2021).

The procedure is to first calculate the isotopologue amount fraction in the standards. Applying the method described in (Griffith, 2018) to CH_4, the isotope ratios are calculated from the isotope ratio assigned to the parent CH_4 – for example, by IRMS measurement.

$$^{13}r = {}^{13}r_{\text{ref}}(1 + \delta^{13}\text{C}), \tag{4}$$

$$^{2}r = {}^{2}r_{\text{ref}}\left(1 + \delta\ {}^{2}\text{H}\right), \tag{5}$$

The mole fractions of the three major isotopologues are then calculated from:

$$X_{211} = \frac{1}{R_{\text{sum}}} \tag{6}$$

$$X_{311} = \frac{r_{13}}{R_{\text{sum}}} \tag{7}$$

$$X_{212} = \frac{4\,r_2}{R_{\text{sum}}} \tag{8}$$

Where $R_{\text{sum}} = \left(1 + {}^{13}r\right)\left(1 + {}^{2}r\right)^4$. The amount fraction in the PRMs (i = low or i = high) are then calculated from:

$$Y^i_{211} = X^i_{211}\,Y^i \tag{9}$$

$$Y^i_{311} = X^i_{311}\,Y^i \tag{10}$$

$$Y^i_{212} = X^i_{212}\,Y^i \tag{11}$$

Where Y^i the total CH_4 amount fraction assigned to the PRM after gravimetric preparation. The PRMs used to evaluate this technique are listed below in Table 1 and are prepared following the protocols described in section 0. These PRMs will bracket the amount fraction of an ambient air sample after preconcentration, and the N_2 matrix will match the composition of the sample as the pre-concentrator has removed O_2 and other gases.

Table 1 Composition of the primary reference materials used to calibrate measurements on the NPL spectrometer using the isotopologue amount fraction method.

Cylinder	Designation	CH_4 / μmol mol^{-1}	$\delta\ ^{13}C$ (CH_4) / ‰	$\delta\ ^{2}H$ (CH_4) / ‰
D049795	Low reference	500.480 ± 0.50	−39.19 ± 0.10	−194.52 ± 1.45
D914016	High reference	620.134 ± 0.62	−39.19 ± 0.10	−194.52 ± 1.45

The amount fraction of the isotopologues in a sample are then calibrated by linear interpolation of the PRMs by a weighted average of the amount fraction of the low and high PRMs

$$Y_j^{\text{samp}} = \left(1 - \alpha_j\right) \mathrm{Y}_\mathrm{j}^{\text{low}} + \alpha_\mathrm{j}\, Y_j^{\text{high}} \tag{12}$$

where the subscript j represents the isotopologues 211, 311 and 212. The weighting for each is given by the instrument response to the sample relative to that of the standards:

$$\alpha_j = \frac{R_j^{samp} - R_j^{low}}{R_j^{high} - R_j^{low}} \quad (13)$$

The isotopologue ratios of the sample are then calculated from the calibrated amount fractions using equations (1) and (2).

3.2 Isotopologue ratio calibration

The optical spectrometer employed at Empa is an upgraded version of the dual-QCL instrument (QCL-76-D, Aerodyne Research Inc., USA) with a multi-pass cell (76 m optical path length, 0.5 L volume) and a pair of continuous-wave DFB-QCL emitting at 1295.7 cm^{-1} and 1307.0 cm^{-1} (Eyer et al., 2016). For instrument calibration the so-called "isotopologue-ratio calibration approach" was applied using CH_4 in N_2 gas standards provided by NPL and VSL (Table 2). The N_2 gas matrix for calibration standards was selected as it represents the target composition after CH_4 preconcentration, i.e., quantitative separation of other atmospheric constituents (e.g., O_2, Ar, N_2O). In case, preconcentrated CH_4 in N_2 contains traces of other gases this may lead to deviations in apparent delta values. The effect of individual permanent (O_2, Ar, Kr) and trace gases (N_2O, H_2O) was tested, and exemplary results are shown in sections 0 and 0. The uncertainty contribution can be estimated from the maximum amount fraction of a component after preconcentration (e.g., < 0.5% for O_2) and its effect on delta values. Currently available gas standards for δ ^{13}C (CH_4) cover ambient CH_4 isotopic composition and enable two-point calibration. For δ ^{2}H (CH_4), however, the spread of isotopic signature in the pure CH_4 sources available to prepare the PRMs is insufficient to retrieve a calibration span with sufficient accuracy.

Table 2 CH_4 isotope reference materials provided by VSL and NPL for OIRS calibration at Empa

	ID	CH4 / µmol mol−1	δ 13C (CH4) / ‰	δ 2H (CH4) / ‰
	112990	2040.0	−47.13 ± 0.22	−191.98 ± 1.06
VSL [1)]	112991	601.7	−45.93 ± 0.19	−190.36 ± 0.78
	112992	569.0	−61.82 ± 0.19	−193.96 ± 0.75
NPL [2)]	10282	10000	−39.19 ± 0.10	−194.5 ± 1.45

1) Analysed by MPI Jena, Feb. 2023. All data is on the JRAS-M16 scale which is directly linked to VPDB in case of d13C, and to VSMOW/SLAP in case of d2H. Uncertainties are standard deviations for replicate measurements (n=4).

2) Pure CH_4 used to prepare cylinder 10282 was analysed by MPI Jena, July 2022.

3.3 Validation of isotope ratio measurement by OIRS

This analysis has been conducted using PRMs prepared with a nominal amount fraction of 550 µmol mol^{-1} using fossil CH_4 from two distinct sources. The isotope ratio of these source methane samples have been measured by IRMS, which is used as the reference value. The mixtures were measured directly on the NPL Aerodyne spectrometer (no preconcentration) using the PRMs listed in Table 1 as calibration standards. Fossil CH_4 sample A is the same source used for the calibration standards and sample B is also from a high-purity fossil fuel source, but with a different δ ^{13}C (CH_4). The spectrometer is optimised for preconcentrated samples, so these mixtures are also prepared at a nominal amount fraction of 550 µmol mol^{-1}, which is near the centre of the calibration range. A complete measurement cycle was performed for each analysis, where the spectrometer cell was evacuated then filled to a target pressure of 2800 Pa and the fitted spectrum averaged for 100 s. These measurements are made as part of the normal operating cycle, so are performed hourly and the results are plotted in Figure 7.

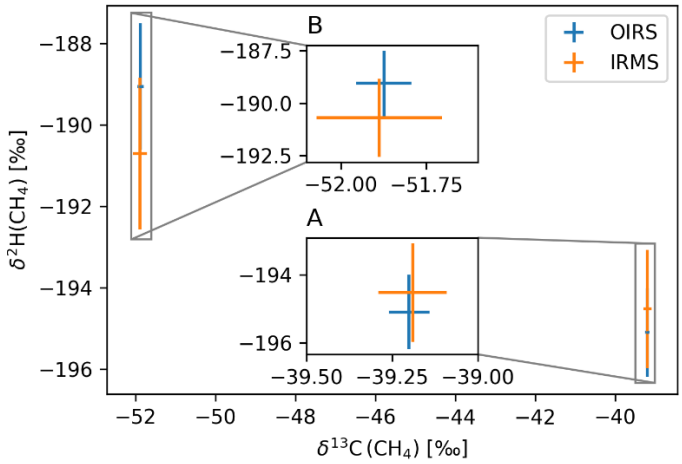

Figure 7 Comparison of isotope ratio measurement of two fossil methane samples by OIRS (blue marker) and IRMS (orange markers), the length of the error bars is the standard deviation of 26 repeated measurements for the OIRS and the mean $\boldsymbol{k} = \mathbf{1}$ uncertainty for IRMS. The inset axes are a zoom into the highlighted boxes.

The mean and standard deviation of the 26 measurements by OIRS are compared with the IRMS results in Table 3. The observed differences are within the range of interlaboratory differences identified by comparison exercises (Umezawa et al., 2018).

Table 3 Isotope ratios of fossil fuel derived CH_4 from two independent sources measured by IRMS and OIRS. The value is the mean of repeated measurements, and the uncertainty is the standard deviation. $\delta\,^2H\,(CH_4)$ was not measured by IRMS for sample B.

	IRMS		OIRS	
CH_4 source	$\delta\,^{13}C\,(CH_4)$ / ‰	$\delta\,^2H\,(CH_4)$ / ‰	$\delta\,^{13}C\,(CH_4)$ / ‰	$\delta\,^2H\,(CH_4)$ / ‰
Fossil A	−39.19 ± 0.10	−194.52 ± 1.45	−39.20 ± 0.06	−195.09 ± 1.09
Fossil B	−51.89 ± 0.18	−190.70 ± 1.85	−51.87 ± 0.08	−189.06 ± 1.55

4 Sample and PRM handling recommendations

4.1 Availability of High purity CH_4 sources for calibration mixtures

The calibration procedures described in section 3 require reference materials with different CH_4 amount fractions and isotopic compositions near the sample values. Deliverable D3 (WP2) provides an extensive description of the work carried out to prepare CH_4 reference materials.

One limitation to the optical measurements after preconcentration is the availability of high amount fraction PRMs in a N_2 matrix. Instruments measuring near-ambient amount fraction also require PRMs with specific composition. The preparation of such mixtures by gravimetric addition of gases (described in section 0) necessitates the use of high purity CH_4, which is predominantly available from fossil sources with a significantly different isotopic composition to background air or other emission sources, such as those listed in Table 4.

Table 4 Isotopic composition of CH_4 in background air and most prominent source processes to guide development of reference materials for calibration of isotope ratio measurements. Average and observed ranges are taken from (Menoud et al., 2022).

CATEGORY	δ ^{13}C (CH_4) / ‰	δ ^{2}H (CH_4) / ‰
Background air	−47.7 ± 0.21	−84.2 ± 5.2
Agriculture	−68 (−70.6 to −46.0)	−319 (−361 to −295)
Waste	−55 (-73.9 to −45.5)	-293 (−312 to −293)
Fossil fuels & non-industrial comb.	−40 (−66.4 to −30.9)	-175 (−199 to −175)
Other anthropogenic sources	−35 (−60 to −9)	-175 (−175 to −81)
Natural wetlands	−69 (−88.9 to −51.5)	-330 (−358 to −246)

For δ ^{13}C (CH_4) alone, ambient composition can in principle be reached by mixing fossil with biogenic (agricultural) CH_4, and Figure 8 shows the potential isotopic compositions that are obtainable with such a mixture. The range of isotopic signatures that can be reached from such a mixture is approximately equal to the average of the pure isotopic signatures weighted by the relative amount fraction.

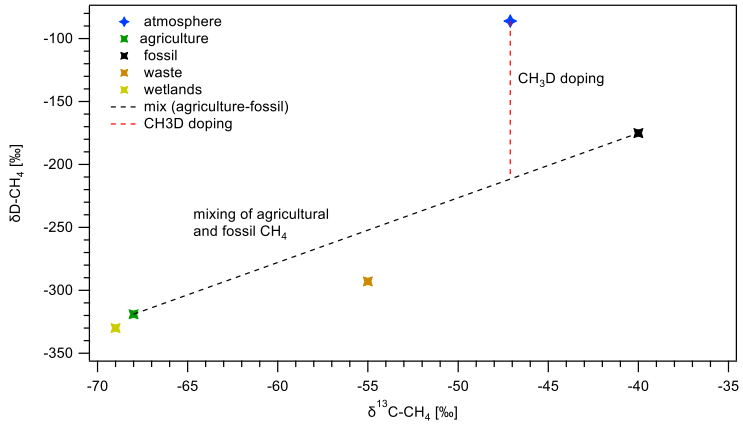

Figure 8 Mixing of CH_4 from agricultural and fossil sources can be used to adjust δ ^{13}C (CH_4) and δ ^{2}H (CH_4) over a range illustrated by the dotted line with the pure sources as endpoints. While a targeted δ ^{13}C (CH_4) that matches atmospheric CH_4 can be reached in principle, δ ^{2}H (CH_4) will always be more negative than an atmospheric sample.

The isotopic signature can be changed by spiking with small amounts of CH_4 that has been enriched in one of the isotopologues. For example, to enhance δ ^{2}H (CH_4) from −216‰ to a target value of −85‰, requires spiking 10 L of the starting material with 0.81 mL pure $^{13}CH_3{}^{2}H$. This change to the composition, however, is not in equilibrium over the minor isotopologues and the OIRS calibration techniques described above assume this equilibrium. This can produce measurement differences between IRMS and OIRS as IRMS measurements are performed after combustion, so the $^{13}C/^{12}C$ ratio is for all isotopologues, while OIRS directly measures the ratio of $^{12}CH_4/^{13}CH_4$ isotopologues. This difference is illustrated in Table 5 for the idealised case of spiking a sample of fossil CH_4 with pure isotopologues $^{12}CH_4$, $^{13}CH_4$ and $^{12}CH_3D$ to replicate isotopic signature near those of distinct sources. The spike amount is the mole fraction of the pure isotopologue, and the balance is the stock fossil CH_4. In general spiking to target an emission source produces a difference between OIRS and IRMS below the uncertainty of the measurement technique. However, the spike required to produce an isotopic signature near ambient air from fossil-source CH_4 may produce measurable differences between the techniques.

TARGET CATEGORY	SPIKE AMOUNT			SPECTROSCOPY		IRMS		DIFFERENCE IRMS - SPEC	
	$^{12}CH_4$	$^{13}CH_4$	$^{12}CH_3D$	$\delta(^{13}CH_4)$	$\delta(^{12}CH_3D)$	$\delta(^{13}C)$	$\delta(D)$	$\delta(^{13}C)$	$\delta(D)$
STOCK	0	0	0	−39.190	−194.520	−39.190	−194.520	0.0	0.0
ATMOSPHERE	8.83×10^{-3}	0.0	7.30×10^{-5}	−47.700	−84.200	−47.765	−85.453	−0.065	−1.253
BIOGENIC	0.14901	0.00140	0.0	−55.000	−300.000	−54.993	−299.843	0.007	0.157
AGRICULTURE	0.18076	0.00156	0.0	−68.000	−319.000	−67.988	−318.743	0.012	0.257
WETLAND	0.2000	0.0018	0.0	−69.000	−330.000	−68.988	−329.736	0.012	0.263

Table 5 Calculated isotope ratio that would be measured by OIRS and IRMS for a sample of pure fossil-source CH_4 that has been spiked with small amounts of the pure isotopologues. The spike amount is the mole fraction of the isotopologue with the balance as the stock CH_4 in the first row.

4.2 IRMS analysis of High purity CH_4 sources for calibration mixtures

PRMs intended for use as calibration gases in OIRS need to be traceable to the internationally accepted references for $\delta\,^{13}C$ and $\delta\,^{2}H$ – VPDB and VSMOW respectively (Sperlich et al., 2016, 2021). This traceability is established by measurement of $\delta\,^{13}C$ and $\delta\,^{2}H$ by IRMS in the high-purity parent CH_4 gases. In the absence of fractionation during preparation this characterisation needs to be performed only once, then all derived PRMs will have a traceable isotopic signature.

Pure CH_4 reference gases used in the Stellar project have been analysed with MPI-BGC HTC and EA systems as described in (Sperlich et al., 2016, 2021). The system provides more flexibility with respect to isotopic composition of CH_4 isotope RMs but for optimal results coverage with international standards is desirable. The applied standards are VSMOW2 (0‰ ± 0.3‰) and SLAP2 (–427.5‰ ± 0.3‰) for $\delta\,^{2}H$ (CH_4) and IAEA-603 (2.46‰ ± 0.01‰) and USGS44 (–42.21‰ ± 0.05‰) for $\delta\,^{13}C$ (CH_4).

A single source of high-purity CH_4 has been identified within the Stellar project. This was supplied by Air Liquide in a 5 L Aluminium high pressure tank containing 50 bar of pure (> 99.9995%) CH_4 (identification H-51160) to the BGC-IsoLab. All measurements are made relative to internationally accepted standards or in-house standards that have been scaled to internationally accepted standards. Each isotopic measurement was done twice, on two separate occasions. A two-point linear normalisation scheme is used to scale all measurements to the respective isotope scale (Paul et al., 2007). Combined uncertainties (standard deviations, SD) are calculated using the "NIST uncertainty machine" (https://uncertainty.nist.gov/) (Lafarge and Possolo, 2015). The results are summarised in Table 6.

Table 6 Results for the analysis of the Stellar high-purity CH_4 by IRMS

	$\delta\,^{13}C_{VPDB}$ / ‰	SD	$\delta\,^{2}H_{VSMOW\text{-}SLAP}$	SD
DAY 1	−39.11	0.15	−194.0	2.54
DAY 2	−39.03	0.08	−195.0	1.40
AVERAGE	−39.07	0.09	−194.52	1.45

4.3 Preparation of calibration gas mixtures

An advantage to the isotopologue amount fraction calibration method described above is that the calibration gases do not have to bracket the sample in the amount fraction for each isotopologue, but the PRMs can be prepared from any high-purity CH_4 that has been characterised for isotopic composition. For validation, however, an independent gas mixture with different isotopic composition, ideally close to the sample gas, is required. Calibration PRMs have been prepared from the high purity CH_4 with identification H-51160 characterised in the previous section.

4.3.1 Gravimetric PRM preparation

All primary reference materials (PRMs) were prepared by gravimetry, in accordance with ISO 6142-1:2015 in 10 L cylinders with BS341 no.14 or BS341 no.15 outlet diaphragm valves. The cylinders were provided by Air Liquide with Aculife III-Megalong internal surface passivation. Cylinders were evacuated using an oil-free pump (Scrollvac SC15D, Leybold Vacuum) and turbo molecular pump with magnetic bearing (Turbo vac 340M, Leybold Vacuum) to a pressure of $< 3 \times 10^{-7}$ mbar.

The reference materials were produced gravimetrically by the addition of CH_4 (Air Liquide, N5.5) of a known isotopic composition via a transfer vessel (100 mL, Luxfer). The transfer vessel was weighed against a tare vessel matched for size and shape before and after CH_4 addition into the evacuated cylinder (Mettler-Toledo XP2004S, ± 0.3 mg). Filling via a transfer vessel was used to achieve a low uncertainty on the addition of small masses. N_2 was added via direct addition, through purged 1/16“ tubing (Swagelok, electro-polished stainless steel) to produce parent reference materials with nominal CH_4 amount fractions of 2000 µmol mol^{-1}. The mass of N_2 added was determined by weighing the cylinder before and after addition against a tare cylinder, using an automatic weighing facility, developed by the Korean Research Institute for Standards and Science (KRISS) (Mettler-Toledo XP26003L, ± 3 mg). The parent amount fraction of 2000 µmol mol^{-1} CH_4 was selected to give the lowest uncertainty in the final 1.95 µmol mol^{-1} CH_4 reference material.

Atmospheric amount fraction reference materials were prepared by the addition of nominally 2000 µmol mol^{-1} reference materials via a transfer vessel into an evacuated 10 L cylinder and dilution with synthetic air by the transfer addition of Kr and direct addition of Ar, O_2 and N_2 at atmospheric amount fractions. Atmospheric amount fraction CH_4 in synthetic air reference materials were prepared with gravimetric combined uncertainties of 0.068% (k=2).

4.4 Gas cylinders and regulators; reducing fractionation at cylinder walls and regulators

Fractionation during storage can be minimised by suitable passivation of all gas-contacting surfaces. The mixtures used here are all prepared in cylinders supplied by Air Liquide with Aculife III-Megalong internal surface passivation. Cylinders were evacuated using an oil-free pump (Scrollvac SC15D, Leybold Vacuum) and turbo molecular pump with magnetic bearing (Turbo vac 340M, Leybold Vacuum) to a pressure of $< 3 \times 10^{-7}$ mbar.

4.5 Preconcentration

Preconcentration is an approach to improving the sensitivity of optical spectroscopy of CH_4 in an air sample by the differences in boiling point (T_{boil}) of the constituent gases. CH_4 (T_{boil} 111 K) will condense on a cooled trapping material packed into tubing while O_2 (T_{boil} 90 K) and N_2 (T_{boil} 77.34 K) flow through (Thermodynamics Research Center, NIST Boulder Laboratories, Chris Muzny director, n.d.). The CH_4 is released by heating the trap with a slower flow rate of N_2 to produce a nominally two-component mixture at a much higher amount fraction. Preconcentrator systems specifically targeting CH_4 have been developed by Empa and NPL and are described in the following sections.

4.5.1 NPL – one-trap preconcentrator

The NPL preconcentrator pumps 5000 mL (STP) of air sample through the cold trap held at approximately −165°C. This allows N_2 and most of the O_2 to pass through while trapping CH_4 and less volatile species. The trap is then used as a chromatographic column by fore-flushing with N_2 while heating with a programmed temperature ramp, separating more volatile species, which leave the trap

and are vented. A valve switches at a timed delay from the start of the temperature ramp and directs the CH_4 sample into the spectrometer before closing again before elution of less volatile species, such as nitrous oxide. The spectrometer is filled to a target pressure corresponding to approximately 18 mL of flushing gas at STP and a nominal preconcentration factor of 278 times. The preconcentrator parameters are optimised by changing the rate of the temperature ramp and the valve timing for transferring the eluant to the spectrometer.

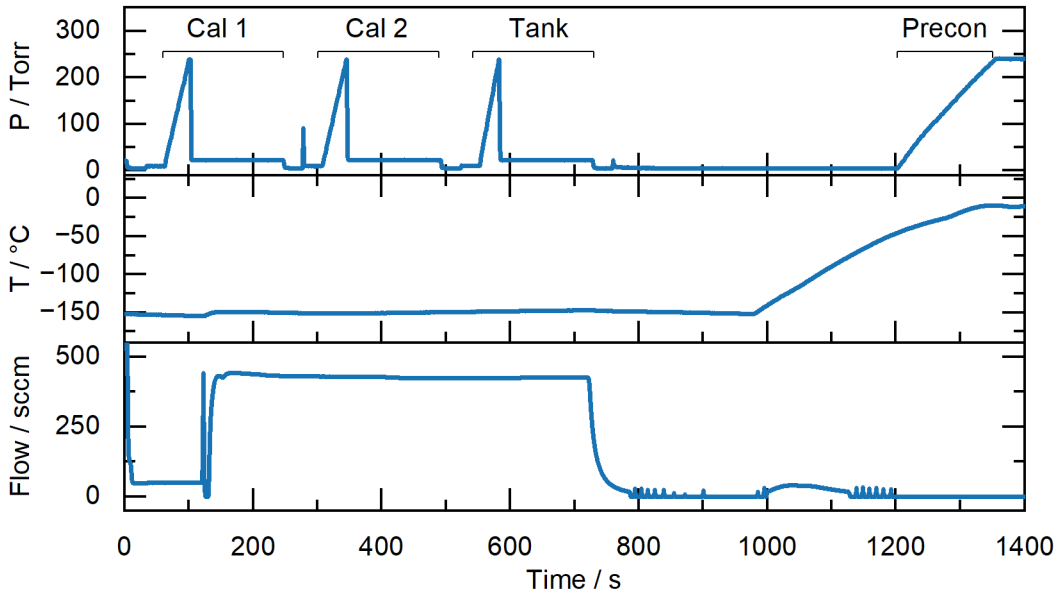

Figure 9 Stripchart of the flow rate through the trap (bottom), the trap temperature (middle), and the pressure in the sample volume used to transfer to the spectrometer (top) during the trapping and elution phases of the sequence. The trap temperature is held low during the trapping phase and then is slowly ramped for elution. The sample volume pressure shows three spikes from loading the two calibration PRMs (cal1, cal2) and one target PRM (tank) into the spectrometer, followed by a pressure increase starting at 1200 s as the eluant is transferred (precon). The air sample flows at around 475 sccm during trapping, followed by a much slower flow of 10 sccm N_2 for the elution and transfer step.

4.5.2 EMPA – two-trap preconcentrator

The Empa system is an upgraded preconcentration device (CleanEx or TREX III), with a second cryofocussing trap (T2). This offers the possibility to remove co-adsorbed O_2 and Ar (T1), which otherwise would lead to changes in the gas matrix, as shown for an earlier version (TREX I) (Eyer *et al.*, 2016). The current performance of TREX III to remove O_2, Ar and CO_2 from CH_4 is shown in Figure 10. The novel preconcentration device was tested for the magnitude of fractionation effects in a series (n = 19) of extraction cycles, where an in-house working reference ($\delta\,^{13}C_{VPDB}$ = −44.21 ± 0.15‰, $\delta\,^{2}H_{VSMOW}$ = −189.0 ± 1‰, 99.9995% CH_4) was dynamically diluted with N_2 in a 1:1000 ratio (1000 µmol mol^{-1} of CH_4) before being processed by CleanEx. The mean observed deviations of −0.1‰, 0.3‰, and −0.3‰ for $\delta\,^{13}C$ (CH_4), $\delta\,^{2}H$ (CH_4), and $\delta\,^{13}CH_3D$, respectively, were within one standard deviation of the measurements, which indicates that fractionation effects are not significant. In comparison with the previously reported preconcentration devices capable of direct deuterated CH_4 measurements, we have achieved almost twofold improvement in uncertainty for $^{12}CH_3D/^{12}CH_4$ and for the first time demonstrated the capability for doubly substituted clumped $^{13}CH_3D$ analysis (Prokhorov and Mohn, 2022).

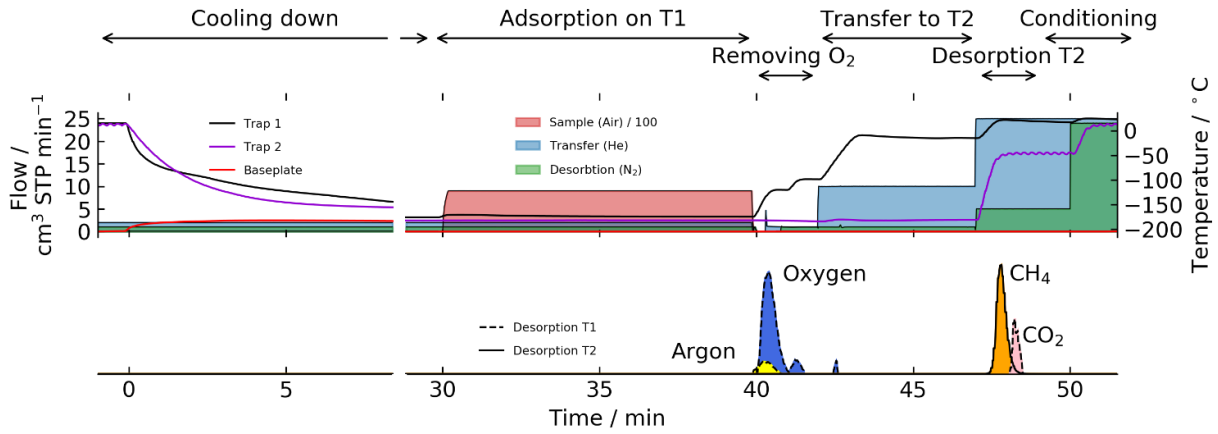

Figure 10 Upper plot: Temperature of adsorbent traps (T1, T2) and baseplate, as well as sample, transfer and desorbant gas flows. Lower plot: Temporal sequence of sequential O_2, Ar, CH_4 and CO_2 desorption from Trap 1 and 2. N_2O was shown to coelute with CO_2.

5 Summary

Measurement of stable isotope ratios in CH_4 with precision 0.2 ‰ for δ ^{13}C (CH_4) and 1 ‰ for δ ^{2}H (CH_4) is possible by OIRS, where this precision is the repeatability of a set of analytical cycles. For atmospheric samples preconcentration is required to increase the amount fraction to around 550 µmol mol^{-1} as current instruments are not capable of achieving this precision at ambient amount fractions. Preconcentration also separates CH_4 from other air components, such as N_2, O_2, Ar, etc., that are also potential interferants. These spectrometers are calibrated using PRMs prepared from a high-purity source of CH_4 that has been characterised for δ ^{13}C (CH_4) and δ ^{2}H (CH_4) by IRMS that is diluted in high purity N_2 to match the matrix of a preconcentrated sample.

6 References

BIPM, IEC, IFCC, ILAC, ISO, IUPAC, IUPAP, and OIML: Evaluation of measurement data — Guide to the expression of uncertainty in measurement, 2008.

BIPM, IEC, IFCC, ILAC, ISO, IUPAC, IUPAP, and OIML: International vocabulary of metrology — Basic and general concepts and associated terms (VIM) 200:2012, 2012.

Canadell, J. G., Scheel Monteiro, P., Costa, M. H., Cotrim da Cunha, L., Cox, P. M., Eliseev, A. V., Henson, S., Ishii, M., Jaccard, S., Koven, C., Lohila, A., Patra, P. K., Piao, S., Rogelj, J., Syampungani, S., Zaehle, S., and Zickfeld, K.: Global carbon and other biogeochemical cycles and feedbacks, in: Climate Change 2021: The Physical Science Basis. Contribution of Working Group I to the Sixth Assessment Report of the Intergovernmental Panel on Climate Change, edited by: Masson-Delmotte, V., Zhai, P., Pirani, A., Connors, S. L., Péan, C., Berger, S., Caud, N., Chen, Y., Goldfarb, L., Gomis, M. I., Huang, M., Leitzell, K., Lonnoy, E., Matthews, J. B. R., Maycock, T. K., Waterfield, T., Yelekçi, Ö., Yu, R., and Zhou, B., Cambridge University Press, 2021.

Eyer, S., Tuzson, B., Popa, M. E., van der Veen, C., Röckmann, T., Rothe, M., Brand, W. A., Fisher, R., Lowry, D., Nisbet, E. G., Brennwald, M. S., Harris, E., Zellweger, C., Emmenegger, L., Fischer, H., and Mohn, J.: Real-time analysis of $\delta^{13}C$- and δD- CH_4 in ambient air with laser spectroscopy: method

development and first intercomparison results, Atmos. Meas. Tech., 9, 263–280, https://doi.org/10.5194/amt-9-263-2016, 2016.

Flores, E., Viallon, J., Moussay, P., Griffith, D. W. T., and Wielgosz, R. I.: Calibration Strategies for FT-IR and Other Isotope Ratio Infrared Spectrometer Instruments for Accurate $\delta^{13}C$ and $\delta^{18}O$ Measurements of CO_2 in Air, Anal. Chem., 89, 3648–3655, https://doi.org/10.1021/acs.analchem.6b05063, 2017.

Gordon, I. E., Rothman, L. S., Hargreaves, R. J., Hashemi, R., Karlovets, E. V., Skinner, F. M., Conway, E. K., Hill, C., Kochanov, R. V., Tan, Y., Wcisło, P., Finenko, A. A., Nelson, K., Bernath, P. F., Birk, M., Boudon, V., Campargue, A., Chance, K. V., Coustenis, A., Drouin, B. J., Flaud, J. –M., Gamache, R. R., Hodges, J. T., Jacquemart, D., Mlawer, E. J., Nikitin, A. V., Perevalov, V. I., Rotger, M., Tennyson, J., Toon, G. C., Tran, H., Tyuterev, V. G., Adkins, E. M., Baker, A., Barbe, A., Canè, E., Császár, A. G., Dudaryonok, A., Egorov, O., Fleisher, A. J., Fleurbaey, H., Foltynowicz, A., Furtenbacher, T., Harrison, J. J., Hartmann, J. –M., Horneman, V. –M., Huang, X., Karman, T., Karns, J., Kassi, S., Kleiner, I., Kofman, V., Kwabia–Tchana, F., Lavrentieva, N. N., Lee, T. J., Long, D. A., Lukashevskaya, A. A., Lyulin, O. M., Makhnev, V. Yu., Matt, W., Massie, S. T., Melosso, M., Mikhailenko, S. N., Mondelain, D., Müller, H. S. P., Naumenko, O. V., Perrin, A., Polyansky, O. L., Raddaoui, E., Raston, P. L., Reed, Z. D., Rey, M., Richard, C., Tóbiás, R., Sadiek, I., Schwenke, D. W., Starikova, E., Sung, K., Tamassia, F., Tashkun, S. A., Vander Auwera, J., Vasilenko, I. A., Vigasin, A. A., Villanueva, G. L., Vispoel, B., Wagner, G., Yachmenev, A., and Yurchenko, S. N.: The HITRAN2020 molecular spectroscopic database, J. Quant. Spectrosc. Radiat. Transfer, 277, 107949, https://doi.org/10.1016/j.jqsrt.2021.107949, 2022.

Griffith, D. W. T.: Calibration of isotopologue-specific optical trace gas analysers: A practical guide, Atmos. Meas. Tech., 11, 6189–6201, https://doi.org/10.5194/amt-2018-187, 2018.

Griffith, D. W. T., Deutscher, N. M., Caldow, C., Kettlewell, G., Riggenbach, M., and Hammer, S.: A Fourier transform infrared trace gas and isotope analyser for atmospheric applications, Atmos. Meas. Tech., 5, 2481–2498, https://doi.org/10.5194/amt-5-2481-2012, 2012.

Lafarge, T. and Possolo, A.: The NIST Uncertainty Machine, NCSLI Measure, 10, 20–27, https://doi.org/10.1080/19315775.2015.11721732, 2015.

Menoud, M., van der Veen, C., Lowry, D., Fernandez, J. M., Bakkaloglu, S., France, J. L., Fisher, R. E., Maazallahi, H., Stanisavljević, M., Nęcki, J., Vinkovic, K., Łakomiec, P., Rinne, J., Korbeń, P., Schmidt, M., Defratyka, S., Yver-Kwok, C., Andersen, T., Chen, H., and Röckmann, T.: Global inventory of the stable isotopic composition of methane surface emissions, augmented by new measurements in Europe, Earth Syst. Sci. Data, 14, 4365–4386, https://doi.org/10.5194/essd-14-4365-2022, 2022.

Miles, N. L., Martins, D. K., Richardson, S. J., Rella, C. W., Arata, C., Lauvaux, T., Davis, K. J., Barkley, Z. R., McKain, K., and Sweeney, C.: Calibration and field testing of cavity ring-down laser spectrometers measuring CH_4, CO_2, and $\delta^{13}CH_4$ deployed on towers in the Marcellus Shale region, Atmos. Meas. Tech., 11, 1273–1295, https://doi.org/10.5194/amt-11-1273-2018, 2018.

Miller, J. B., Mack, K. A., Dissly, R., White, J. W. C., Dlugokencky, E. J., and Tans, P. P.: Development of analytical methods and measurements of $^{13}C/^{12}C$ in atmospheric CH_4 from the NOAA Climate Monitoring and Diagnostics Laboratory Global Air Sampling Network, J. Geophys. Res. Atmos., 107, ACH 11-1-ACH 11-15, https://doi.org/10.1029/2001JD000630, 2002.

Nisbet, E. G., Dlugokencky, E. J., Manning, M. R., Lowry, D., Fisher, R. E., France, J. L., Michel, S. E., Miller, J. B., White, J. W. C., Vaughn, B., Bousquet, P., Pyle, J. A., Warwick, N. J., Cain, M., Brownlow,

R., Zazzeri, G., Lanoisellé, M., Manning, A. C., Gloor, E., Worthy, D. E. J., Brunke, E.-G., Labuschagne, C., Wolff, E. W., and Ganesan, A. L.: Rising atmospheric methane: 2007-2014 growth and isotopic shift, Global Biogeochem. Cycles, 30, https://doi.org/10.1002/2016GB005406, 2016.

Nisbet, E. G., Manning, M. R., Dlugokencky, E. J., Fisher, R. E., Lowry, D., Michel, S. E., Myhre, C. L., Platt, S. M., Allen, G., Bousquet, P., Brownlow, R., Cain, M., France, J. L., Hermansen, O., Hossaini, R., Jones, A. E., Levin, I., Manning, A. C., Myhre, G., Pyle, J. A., Vaughn, B., Warwick, N. J., and White, J. W. C.: Very strong atmospheric methane growth in the four years 2014-2017: Implications for the Paris Agreement, Global Biogeochem. Cycles, 33, 318–342, https://doi.org/10.1029/2018GB006009, 2019.

Paul, D., Skrzypek, G., and Fórizs, I.: Normalization of measured stable isotopic compositions to isotope reference scales – a review, Rapid Commun. Mass Spectrom., 21, 3006–3014, https://doi.org/10.1002/rcm.3185, 2007.

Prokhorov, I. and Mohn, J.: CleanEx: A Versatile Automated Methane Preconcentration Device for High-Precision Analysis of $^{13}CH_4$, $^{12}CH_3D$, and $^{13}CH_3D$, Anal. Chem., 94, 9981–9986, https://doi.org/10.1021/acs.analchem.2c01949, 2022.

Rella, C. W., Hoffnagle, J., He, Y., and Tajima, S.: Local- and regional-scale measurements of CH_4, $\delta\ ^{13}CH_4$, and C_2H_6 in the Uintah Basin using a mobile stable isotope analyzer, Atmos. Meas. Tech., 8, 4539–4559, https://doi.org/10.5194/amt-8-4539-2015, 2015.

Rennick, C., Arnold, T., Safi, E., Drinkwater, A., Dylag, C., Webber, E. M., Hill-Pearce, R., Worton, D. R., Bausi, F., and Lowry, D.: Boreas: A Sample Preparation-Coupled Laser Spectrometer System for Simultaneous High-Precision In Situ Analysis of $\delta\ ^{13}C$ and $\delta\ ^{2}H$ from Ambient Air Methane, Anal. Chem., 93, 10141–10151, https://doi.org/10.1021/acs.analchem.1c01103, 2021.

Röckmann, T., Eyer, S., van der Veen, C., Popa, M. E., Tuzson, B., Monteil, G., Houweling, S., Harris, E., Brunner, D., Fischer, H., Zazzeri, G., Lowry, D., Nisbet, E. G., Brand, W. A., Necki, J. M., Emmenegger, L., and Mohn, J.: In situ observations of the isotopic composition of methane at the Cabauw tall tower site, Atmos. Chem. Phys., 16, 10469–10487, https://doi.org/10.5194/acp-16-10469-2016, 2016.

Saboya, E., Zazzeri, G., Graven, H., Manning, A. J., and Englund Michel, S.: Continuous CH_4 and $\delta^{13}CH_4$ measurements in London demonstrate under-reported natural gas leakage, Atmos. Chem. Phys., 22, 3595–3613, https://doi.org/10.5194/acp-22-3595-2022, 2022.

Santoni, G. W., Lee, B. H., Goodrich, J. P., Varner, R. K., Crill, P. M., McManus, J. B., Nelson, D. D., Zahniser, M. S., and Wofsy, S. C.: Mass fluxes and isofluxes of methane (CH_4) at a New Hampshire fen measured by a continuous wave quantum cascade laser spectrometer, J. Geophys. Res. Atmos., 117, https://doi.org/10.1029/2011JD016960, 2012.

Sperlich, P., Uitslag, N. A. M., Richter, J. M., Rothe, M., Geilmann, H., van der Veen, C., Röckmann, T., Blunier, T., and Brand, W. A.: Development and evaluation of a suite of isotope reference gases for methane in air, Atmos. Meas. Tech., 9, 3717–3737, https://doi.org/10.5194/amt-9-3717-2016, 2016.

Sperlich, P., Moossen, H., Geilmann, H., Bury, S. J., Brown, J. C. S., Moss, R. C., Brailsford, G. W., and Brand, W. A.: A robust method for direct calibration of isotope ratios in gases against liquid/solid reference materials, including a laboratory comparison for $\delta^{13}C$-CH_4, Rapid Commun. Mass Spectrom., 35, e8944, https://doi.org/10.1002/rcm.8944, 2021.

Steur, P. M., Scheeren, H. A., Nelson, D. D., McManus, J. B., and Meijer, H. A. J.: Simultaneous measurement of δ ^{13}C, δ ^{18}O and δ ^{17}O of atmospheric CO_2 – performance assessment of a dual-laser absorption spectrometer, Atmos. Meas. Tech., 14, 4279–4304, https://doi.org/10.5194/amt-14-4279-2021, 2021.

Thermodynamics Research Center, NIST Boulder Laboratories, Chris Muzny director: Thermodynamics Source Database, in: NIST Chemistry WebBook, NIST Standard Reference Database Number 69, National Institute of Standards and Technology, Gaithersburg MD, 20899, n.d.

Umezawa, T., Brenninkmeijer, C. A. M., Röckmann, T., van der Veen, C., Tyler, S. C., Fujita, R., Morimoto, S., Aoki, S., Sowers, T., Schmitt, J., Bock, M., Beck, J., Fischer, H., Michel, S. E., Vaughn, B. H., Miller, J. B., White, J. W. C., Brailsford, G., Schaefer, H., Sperlich, P., Brand, W. A., Rothe, M., Blunier, T., Lowry, D., Fisher, R. E., Nisbet, E. G., Rice, A. L., Bergamaschi, P., Veidt, C., and Levin, I.: Interlaboratory comparison of δ ^{13}C and δ D measurements of atmospheric CH_4 for combined use of data sets from different laboratories, Atmos. Meas. Tech., 11, 1207–1231, https://doi.org/10.5194/amt-11-1207-2018, 2018.

Werle, P.: Accuracy and precision of laser spectrometers for trace gas sensing in the presence of optical fringes and atmospheric turbulence, Appl. Phys. B, 102, 313–329, https://doi.org/10.1007/s00340-010-4165-9, 2011.

Werle, P., Mücke, R., and Slemr, F.: The limits of signal averaging in atmospheric trace-gas monitoring by tunable diode-laser absorption spectroscopy (TDLAS), Appl. Phys. B, 57, 131–139, https://doi.org/10.1007/BF00425997, 1993.

Werle, P. W., Mazzinghi, P., D'Amato, F., De Rosa, M., Maurer, K., and Slemr, F.: Signal processing and calibration procedures for in situ diode-laser absorption spectroscopy, Spectrochimica Acta Part A: Molecular and Biomolecular Spectroscopy, 60, 1685–1705, https://doi.org/10.1016/j.saa.2003.10.013, 2004.

Werner, R. A. and Brand, W. A.: Referencing strategies and techniques in stable isotope ratio analysis, Rapid Commun. Mass Spectrom., 15, 501–519, https://doi.org/10.1002/rcm.258, 2001.

Appendix A Definitions

An isotope is an atom of the same element with a different mass due to differing number of neutrons. Stable isotopes are those that are stable with respect to nuclear decay. Of the elements in CH_4 the stable isotopes of carbon are ^{12}C and ^{13}C and the stable isotopes of hydrogen are ^{1}H and ^{2}H (also named deuterium with symbol D).

An isotopologue is an isotopic analogue of a molecule, where one or more isotopes have been substituted.

The precision of a laser spectroscopic measurement is often evaluated and reported using the "Allan variance" concept developed by Peter Werle (Werle et al., 1993, 2004; Werle, 2011). In this concept, noise is considered as the sum of frequency independent (white) noise and low frequency noise, called drift. An Allan plot provides the Allan variance, and its square root provides the Allan precision as a function of measurement time. At low integration times, white noise dominates and the precision increases proportionally to the integration time. Beyond the optimum integration time drift begins to dominate.

The repeatability of results indicates the closeness of the agreement between successive measurements of the same measurand carried out under the same measurement conditions (BIPM et al., 2012). Repeatability conditions include the same instrument, observer, measurement conditions and procedure and reference standard. Repeatability may be expressed quantitatively in terms of dispersion characteristics of the results.

The reproducibility of results indicates the closeness of the agreement between results of measurements of the same measurand carried out under changed measurement conditions (BIPM et al., 2012). Changed conditions may include a different instrument, observer, measurement principle and method etc. Reproducibility may be expressed quantitatively in terms of dispersion characteristics of results.

The measurement uncertainty characterizes the dispersion of the values that could be attributed to the measurand (BIPM et al., 2012). The standard uncertainty is the standard deviation of a distribution of measurement values that represent a 68 %-probability of covering the 'true' value. A combined uncertainty is the resulting uncertainty considering an appropriate number of contributing sources of uncertainties associated with those influencing quantities present in the model equation. The expanded uncertainty can be calculated from the (combined) uncertainty by multiplication with a coverage factor, k to encompass a larger probability of covering the 'true' value. The coverage factor $k = 2$ results in a confidence interval of approximately 95%, and $k = 3$ a confidence interval of approximately 99% (BIPM et al., 2008).

An uncertainty comprises many components, which can be partly evaluated from the statistical distribution of results of a series of measurements, characterized by experimental standard deviations (type-A uncertainty). Those components, which can be characterized by other means are evaluated from assumed probability distributions based on experience or other information (type-B uncertainty). If all quantities on which the result depends are varied, its uncertainty can be evaluated by statistical means.

Appendix B Spectral windows for interference-free spectroscopic CH_4 isotope Discrimination

Spectral windows and line data used for the analysis of singly substituted CH_4 isotopic species. Line positions and line strengths given in Table 2 were retrieved from the HITRAN database (Rothman *et al.*, 2005) using wavenumber information provided by instrument manufacturers. Line data of prominent spectral interferants are listed in the supporting information.

Table 7 Spectroscopic windows

Instrument (Institute) Reference	Wavenumber [cm^{-1}]	Isotopic species	Line positions [cm^{-1}] / abundance-weighted line strength [cm^{-1}/ (molecule cm^{-2})]	Reference
Aerodyne (Empa)	1295.6 – 1295.7	211 311	1295.673 / 5.811x10^{-22} 1295.649 / 6.050x10^{-23} 1295.626 / 5.654x10^{-22}	(Eyer *et al.*, 2016)
	1306.9 – 1307.05	211 212 N_2O	1306.948 / 9.273x10^{-23} 1307.040 / 2.229x10^{-23} 1306.929 / 1.040x10^{-19}	
Aerodyne (NPL)	1293.702 – 1293.814	211 311	1293.781 / 4.482×10^{-22} 1293.716 / 4.129×10^{-22}	
	1306.885-1307.082	212 N_2O H_2O	1307.04 cm^{-1} / 2.22×10^{-23} 1306.929 cm^{-1} / 1.04×10^{-19} 1307.019 cm^{-1} / 6.30×10^{-24}	
Picarro G2201-I (PTB)	6028 – 6058	211 (HP)* 311 211 (HR)*	6057.08 / 1.52×10^{-21} 6029.11 / 1.52×10^{-23} 6028.55 / 2.57x10^{-23}	Dinger (2014) for line position
CRDS (VSL)	2950.8-2951.4 (211 & 311)	211 311	2950.863 / 1.447x10^{-24} 2951.3057 / 1.233x10^{-22} 2950.851 / 2.734x10^{-23} 2951.360 / 1.884x10^{-24}	Hitran: 2951.35955 cm-1 and 2951.35983 cm-1 with same S
	3067.4-3069.0 (211, 311 & 212)	212	3068.95048 / 4.409x10^{-23}	
TDLAS (VTT)	3060.25 – 3060.45	311 211 311 211	3060.320 / 7.20×10^{-24} 3060.363 / 1.38×10^{-23} 3060.377 / 5.10×10^{-24} 3060.408 / 1.20×10^{-24}	(Kääriäinen *et al.*, 2018)
	3061.38 – 3061.53	212 211	3061.414 / 5.08 e^{-23} 3061.494 / 9.64 e^{-23}	

* HP: high precision mode; HR: high amount fraction range

The VTT TDLAS spectrometer is targeting samples from CH_4 sources with amount fractions above 10 mmol mol^{-1}. In such samples, the strongest interference is expected to originate from other Hydrocarbons (primarily CH_3Cl, C_2H_4, C_3H_8, C_6H_6).